nature communications

Article

https://doi.org/10.1038/s41467-025-63848-7

Design of a combined LED and rapid-injection NMR system for structure elucidations and kinetic analyses

Received: 11 April 2025

Accepted: 1 September 2025

Published online: 02 October 2025

Check for updates

Danniel K. Arriaga, Ravinder Kaur & Andy A. Thomas

Nuclear magnetic resonance (NMR) spectroscopy is a powerful technique often used for structural elucidation of various molecules. The utility of NMR for in situ reaction monitoring is represented by the numerous strategies to conduct chemical reactions inside of the spectrometer, such as rapid-injection (RI-NMR) and LED NMR. In this work, the design of a combined LED and rapid-injection NMR (LED-RI-NMR) apparatus is described and showcased in kinetic studies for three photochemical reactions. The simple design of the LED-RI-NMR system allows for the introduction of both light and reagents into NMR samples for in situ reaction monitoring of reactive intermediates. The distinguishing features of the LED-RI-NMR system described herein include the ability to explore and intercept photogenerated intermediates via RI-NMR and explore the photochemical properties of fleeting intermediates generated by RI-NMR. We demonstrate the versatility of this experimental tool for the kinetic study of organophotoredox cycloadditions, Wolff rearrangements, and azobenzene isomerization reactions.

Nuclear magnetic resonance (NMR) spectroscopy is a foundational physical technique that correlates structural information with both reactivity and selectivity in chemical transformations. While mostly used by chemists for structural elucidation of small and large molecules, the use of internal standards allows for quantitative in situ reaction monitoring to obtain detailed kinetic information[1]. Perhaps unsurprisingly, the advancement of reaction monitoring techniques often coincides with the development of chemical processes and the expansion of existing ones, as these techniques provide the necessary mechanistic insights to navigate the ever-growing chemical landscape. In this regard, NMR spectroscopy continues to disclose the underlying mechanisms of many reactions. However, reactions that have short-lived intermediates ($t_{½} < 1$ s)[2], those that require external stimulation (e.g., illumination), and those that need sufficient mixing to proceed are, from a practical perspective, challenging to study. Various reaction monitoring techniques such as stopped-flow[3], continuous flow[4], rapid-injection NMR (RI-NMR)[5], and illumination NMR have been developed to circumvent several of these practical limitations, thereby expanding the range of reaction systems that can be investigated in real time (Fig. 1A). For example, LED-NMR emerged as a powerful tool in the recent renaissance of visible-light-driven chemical reactions and photoredox catalysis, enabling the study of their underlying mechanisms[6–10]. The incorporation of LEDs with NMR, initially developed by Gschwind[11], was rapidly applied by Lehnherr and Ji, Nicewicz, MacMillan, amongst others, to investigate various light-driven systems[12,13]. Operationally, this was a significant advancement in reaction monitoring as the experimental conditions of organic transformations could be transferred inside the NMR spectrometer without modifying the instrument itself – facilitating widespread adoption of this technique. While LED-NMR setups are powerful tools for studying various chemical processes, current reaction monitoring technologies lack the ability to add additional reagents during the illumination of a sample inside the NMR spectrometer – mimicking the addition of chemical reagents to a flask under illumination. The utility of ReactIR and flash photolysis as reaction monitoring methods circumvents this issue with limited structural information gained[14,15]. The ability to perform such experimentation within the NMR spectrometer would open the door to explore the chemical reactivity of photogenerated intermediates, as well as the photochemical properties of fleeting intermediates. Given that our research program is focused on

Department of Chemistry, Texas A&M University, College Station, TX, USA. e-mail: andythomas@tamu.edu

https://doi.org/10.1038/s41467-025-63848-7

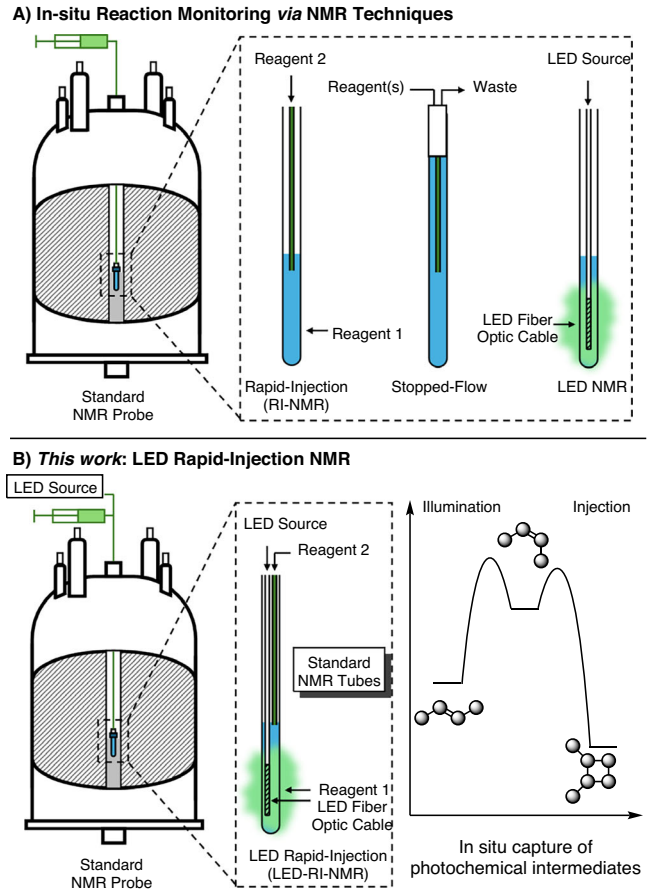

Fig. 1 | NMR techniques for in situ reaction monitoring. A Differentiation between rapid-injection (RI-NMR), stopped-flow, and LED-NMR techniques. RI-NMR utilizes a glass capillary to deliver a second reagent into the NMR tube. Stopped-flow employs a flow-cell NMR tube for reaction monitoring. LED NMR uses a sanded fiber optic cable to introduce light into the NMR tube inside of the spectrometer. **B** This work – LED incorporated RI-NMR (LED-RI-NMR) and potential applications of the system. The LED-RI-NMR system uses a combination of glass capillaries and fiber optic cables to introduce additional reagents and light sequentially or simultaneously.

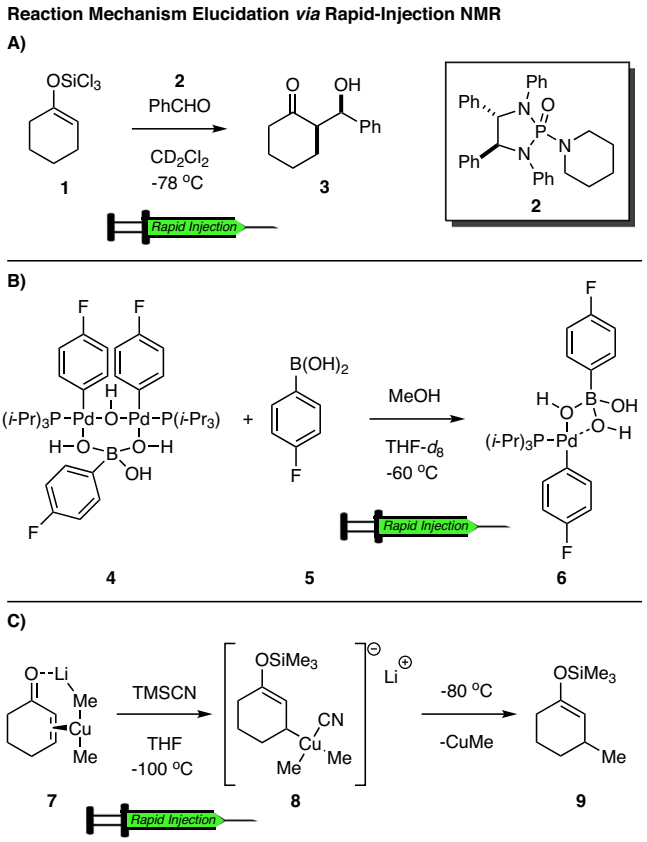

Fig. 2 | Elucidation of reaction mechanisms through rapid-injection NMR spectroscopy (RI-NMR). A Mechanistic studies on Lewis-base catalyzed Aldol additions studied by Denmark. **B** Pre-transmetalation intermediates in the Suzuki-Miyaura reaction studied by Thomas and Denmark. **C** Mechanism studies on conjugate addition reactions with dialkyl cuprates studied by Ogle.

exploring the reactivity of intermediates and the design of RI-NMR techniques, we were inspired to develop a reaction monitoring system that combines LEDs with RI-NMR for mechanistic investigations[16,17]. Herein, we describe the design of an LED-incorporated RI-NMR system (LED-RI-NMR) that enables the interception of photogenerated intermediates via RI-NMR, and investigation of the photochemical properties of fleeting intermediates following their generation by RI-NMR (Fig. 1B). Of note, the tandem illumination injection feature provided by the LED-RI-NMR system circumvents starting material incompatibilities by allowing for the generation of intermediates before other starting reagents are added inside the NMR tube. This in situ generation of sensitive intermediates and their subsequent investigation de facto expands our ability to both discover and optimize reactions. To showcase the utility of the LED-RI-NMR system, we investigated organophotoredox cycloadditions, Wolff rearrangements, and azobenzene isomerization reactions in detail.

Rapid-injection NMR (RI-NMR) spectroscopy is a conceptually simple technique that allows for the in-situ generation and characterization of reactive intermediates inside the NMR spectrometer[18]. Since McGarrity's initial conception of the instruments, the primary focus has been to utilize these reaction monitoring systems as a means of linking structural and kinetic data together – providing a powerful physical organic technique to understand how structure impacts reactivity in real time. For example, later RI-NMR systems developed by Ogle[19], Denmark[5], and Reich[20] have been invaluable in elucidating the mechanisms of several classes of organic transformations: especially, Mukaiyama aldols, Suzuki-Miyaura reactions, as well as organolithium and organocuprate mediated transformations (Fig. 2). Given our interest in mechanism driven method development, we have sought avenues to improve our workflow through the design of RI-NMR systems that mimic reaction conditions performed on the bench, allowing for the mechanistic investigation of reactive intermediates under real life settings. One recent example is the construction of a gas-injector that precisely and reliably introduces gases into the NMR sample for reaction monitoring[21]. This perspective of RI-NMR combined with our interests in photochemistry, inspired us to construct an LED-incorporated RI-NMR system that could serve a dual purpose: (1) introduce light to induce photochemical reactions, and (2) inject additional reagents to capture photochemical intermediates. Herein, we describe the design of such an LED-RI-NMR system in detail and implement the instrument for the study of three light-driven reactions: a photocatalytic [3 + 2]-cycloaddition, a Wolff rearrangement, and a [2 + 2]-cycloaddition of a photostationary state. In these reactions, we demonstrate that both the LED and injector components of the apparatus can be used independently, or simultaneously if needed, to explore reaction mechanisms. By incorporating these features with variable temperature NMR and an internal standard, a myriad of qualitative and quantitative data can be accessed with one tool.

Results & Discussion

Gaining inspiration from the McGarrity, Ogle, Reich, and Denmark RI-NMR systems, our approach was focused on developing an apparatus

https://doi.org/10.1038/s41467-025-63848-7

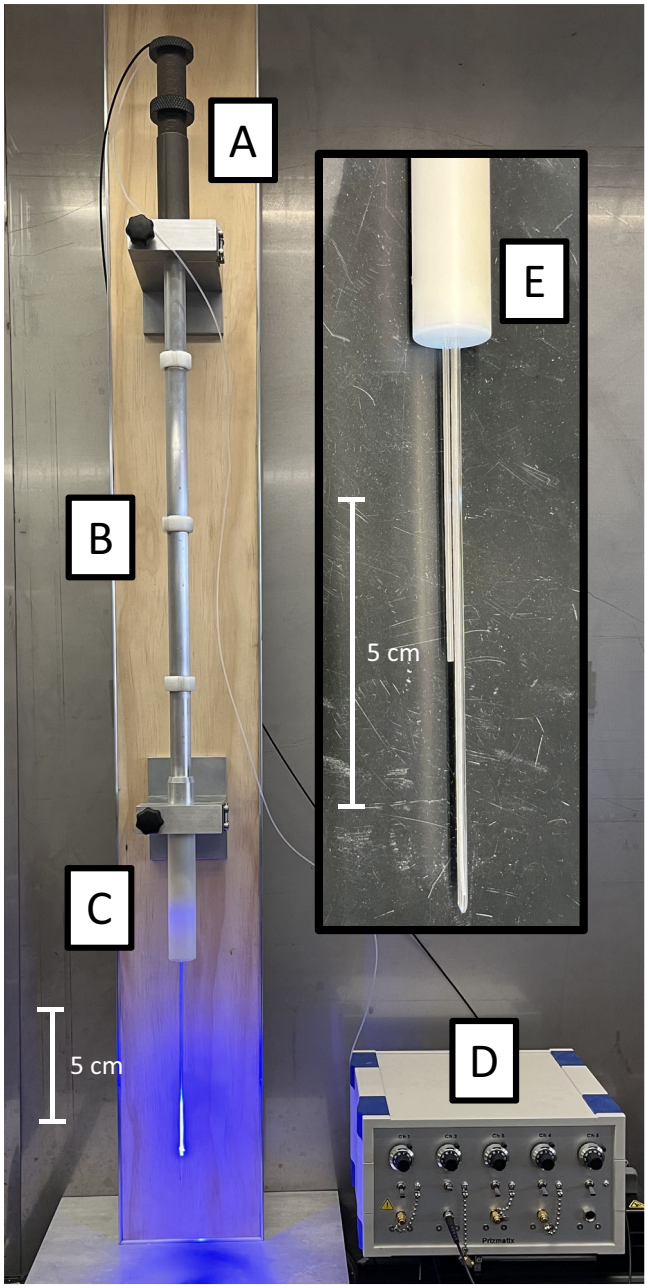

Fig. 3 | LED rapid-injection NMR (LED-RI-NMR) apparatus. A Polyacetal height adjusting handle. **B** Aluminum injector barrel with Teflon spacers. **C** Polyacetal injector tip assembly. **D** Multi-channel LED box. **E** Close-up of Injector tip assembly with injection capillary (left) and LED capillary (right).

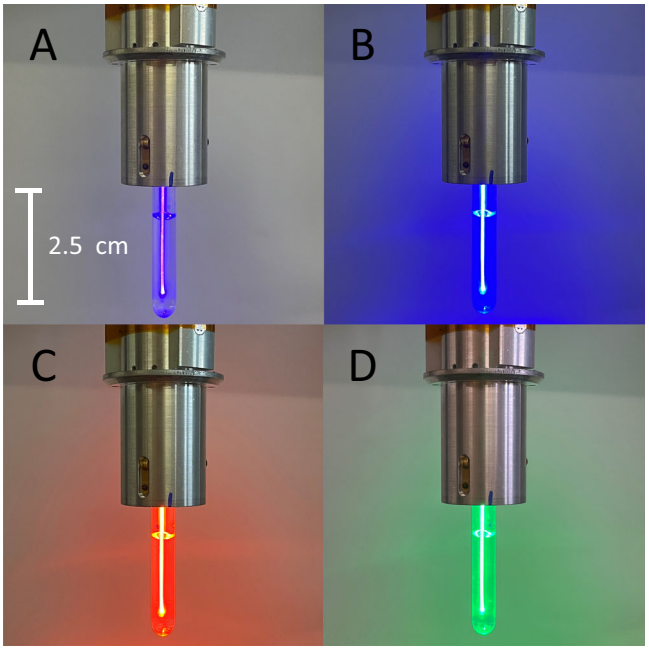

Fig. 4 | Examples of different wavelengths of light equipped with the LED-RI-NMR system. A 402 nm, **B** 454 nm, **C** 524 nm, **D** 631 nm.

that did not require modifications to the NMR spectrometer, probe, or facility[2,22]. We describe below an overview of the LED-RI-NMR system; however, detailed schematics are available in the Supporting Information. The LED-RI-NMR system was adapted for a Varian VNMRS 500 MHz spectrometer equipped with a 10 mm Varian NMR probe. The barrel of the injector was constructed from a hollow aluminum rod 53 cm in length equipped with a height-adjusting handle and injector tip assembly (Fig. 3). The injector tip assembly has two perforations at the bottom fitted with a 3 mm sealed capillary for the fiber optic cable and an open 1 mm capillary for RI-NMR (Fig. 3E). The fiber optic cable was fed through the aluminum rod to a Prizmatix multiple wavelength LED box capable of emitting light from four different wavelengths: (A) 402 nm, (B) 454 nm, (C) 524 nm, and (D) 631 nm (Fig. 4A–D). The injector capillary was connected to a polymer threaded coupling (1/4-28 NPT) equipped with 5.4 mm OD (0.1 mm ID) Teflon O-rings and coupled with Teflon tubing and Tefzel microfluidic ferrules and nuts to a Harvard Apparatus syringe pump. With the LED-RI-NMR system in hand our investigations switched to calibrating the delivery of LEDs, organic media, as well as mixing.

Introducing light into NMR samples presents a challenge; ensuring compatibility with the LED source, associated equipment, and the NMR spectrometer is often arduous. Integrating LEDs into the NMR probe enables simultaneous illumination of various samples and enables rapid-injection experiments. However, this approach requires significant modification to the probe. While placing an LED lamp at the top of the NMR bore is an option, this raises concerns about the efficiency of sample illumination due to the large distance between the lamp and the sample. To address this issue, we sought a method to directly illuminate the sample without modifying the NMR probe or sample tube. Inspired by Gschwind's previous LED-NMR setups[11], we utilized a sanded polycarbonate fiber optic cable encased in a 3 mm sealed glass capillary. This configuration allows for direct illumination of the NMR sample, and since the fiber optic cable is part of the LED-RI-NMR assembly, no modifications to the NMR tube or probe are required for illumination experiments. Additionally, this placement of the fiber optic cable enables uniform illumination of the sample in the measuring coils of the NMR spectrometer (Fig. 5).

A common issue in RI-NMR experiments is the injection of reagents into the sample without early detection. Since the LED-RI-NMR system remains static inside the sample while collecting spectra, it was not feasible to position the injector tip at the same depth as the LED capillary. To avoid early detection of the injected reagent, we explored the idea of raising the injection capillary above the sample. After trial and error, it was found that positioning the injector tip 4 cm above the solution in the NMR tube effectively prevented early detection while enabling successful reagent delivery. This injection system demonstrated a linear range (Fig. 6) of injected volume between 100 and 500 µL (*slope* = 0.9803 ± 0.016).

Often the biggest challenge in RI-NMR experiments is achieving fast and efficient mixing. By submerging the LED capillary in the NMR sample and spinning the NMR tube at 6 Hz, effective mixing of Blue #1 in MeOH (Fig. 7A–D) is rapidly achieved (<1 s) with a 200 µL injection

https://doi.org/10.1038/s41467-025-63848-7

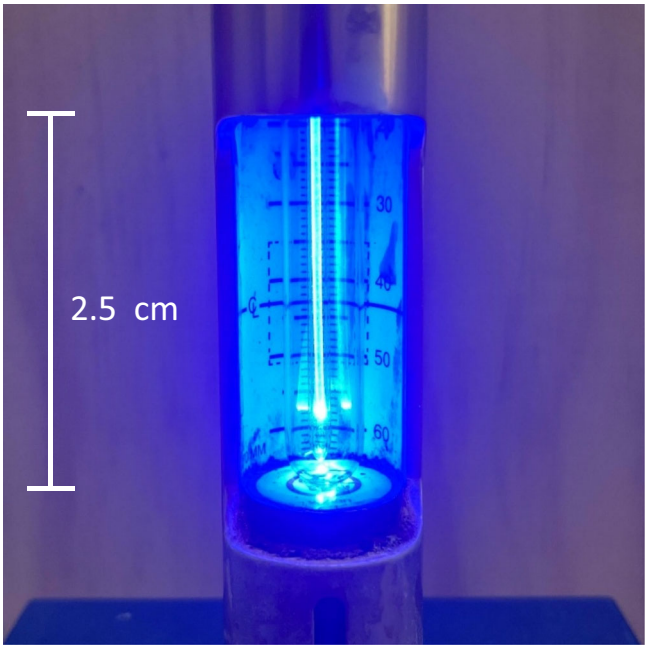

Fig. 5 | Depth gauge for a Varian VNMRS system with a 10 mm tube and LED-RI-NMR capillary inside. Dashed box indicates the location of the measuring coils for the NMR spectrometer.

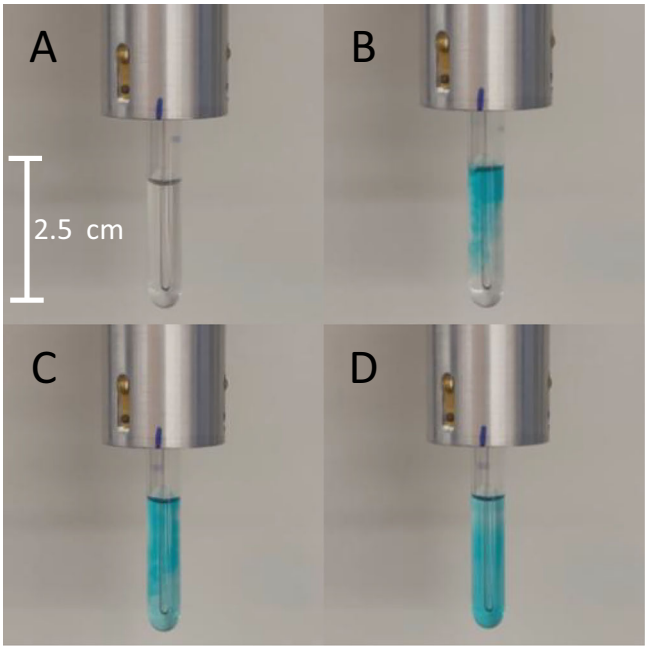

Fig. 7 | Injection of Blue #1 food safe dye in 200 µL of MeOH. A Pre-injection with 2 mL of MeOH in a 10 mm NMR tube spinning at 6 Hz. A video of the injection sequence is available as Supplementary Video 1. Injection at **B** 0.55 s, **C** 1.29 s, and **D** 3.02 s.

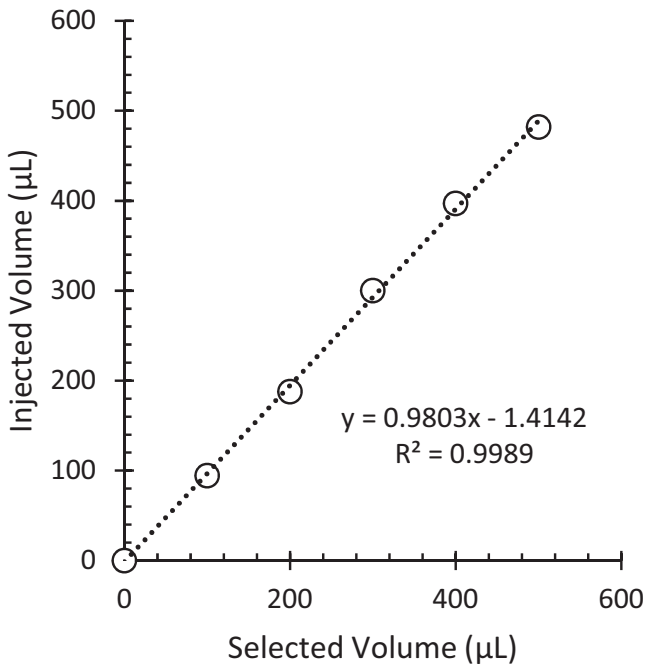

Fig. 6 | Plot of injected volume vs. selected volume on the LED-RI-NMR syringe pump. Injections were performed in 10 mm NMR tubes using 2 mL of THF and injecting between 100 and 500 µL of benzene into the sample.

(See Supplementary Video 1). Key to success in our system was the LED-capillary, which provided a fixed mixer. With the finished injector in hand, we then sought out well-tested and reported reactions to validate the practicality of this spectroscopic tool.

To calibrate the LED-RI-NMR system for mechanistic investigations, we needed to demonstrate its ability to mimic standard bench reaction protocols that require illumination as well as the addition of reagents over a range of temperatures and time frames under inert atmospheres. Of note, the illumination and injection features were designed to be independent from one another and compatible with VT-cooling and heating. Therefore, our efforts became focused on testing: (1) the illumination feature (without rapid injection) by exploring a photocatalytic reaction that has all of the reaction components pre-mixed; (2) the illumination feature in tandem with rapid injection to photogenerate an intermediate and capture it by rapid injection; and (3) the illumination feature in concert with rapid injection to generate and investigate an intermediate under constant irradiation.

The construction of the LED-RI-NMR injector system was initiated in part by our recent interest in photoredox-enabled reactions, wherein we opted to study the photosensitized generation of carbonyl ylides. Carbonyl ylides are a type of 1,3-dipole generated by a variety of methods that react readily with electron-deficient alkenes to form highly substituted tetrahydrofurans[23]. Recently, strategies to generate carbonyl ylides through redox-neutral photocatalysts have allowed for the synthesis of various other small molecules[24,25]. While the direct photolysis of epoxides to carbonyl ylides have been studied, kinetic studies on the photosensitized reactions are scarce and rely on laser flash photolysis instead of bulk solution monitoring[26,27].

We began by combining *trans*-stilbene oxide **10** with citraconic anhydride **11** in benzene-d_6 with the acridinium photocatalyst **12**. The ^{1}H NMR spectra were recorded over a course of 22 h under constant irradiation at 454 nm allowing for the activation of the photocatalyst **12**, decay of starting materials **10** and **11**, as well as the formation of product **13** to be monitored (Fig. 8A). The initiation of **12** into its photoactive state was completed within minutes ($t_{1/2}$ = 11.27 ± 0.19 min) following a first-order kinetic model under constant light intensity[28]. Due to the paramagnetic nature of the active photocatalysts, these intermediates could not be detected by ^{1}H NMR spectroscopy. Of note, the C-C opening of epoxides using photosensitizers is traditionally performed with cyanoarenes as photocatalysts; however, we found that acridinium photocatalysts, such as **12**, are compatible in the desired reaction[19].

The kinetic order dependence in **10, 11**, and **12** was then determined by monitoring the formation of **13** by ^{1}H NMR over a range of

https://doi.org/10.1038/s41467-025-63848-7

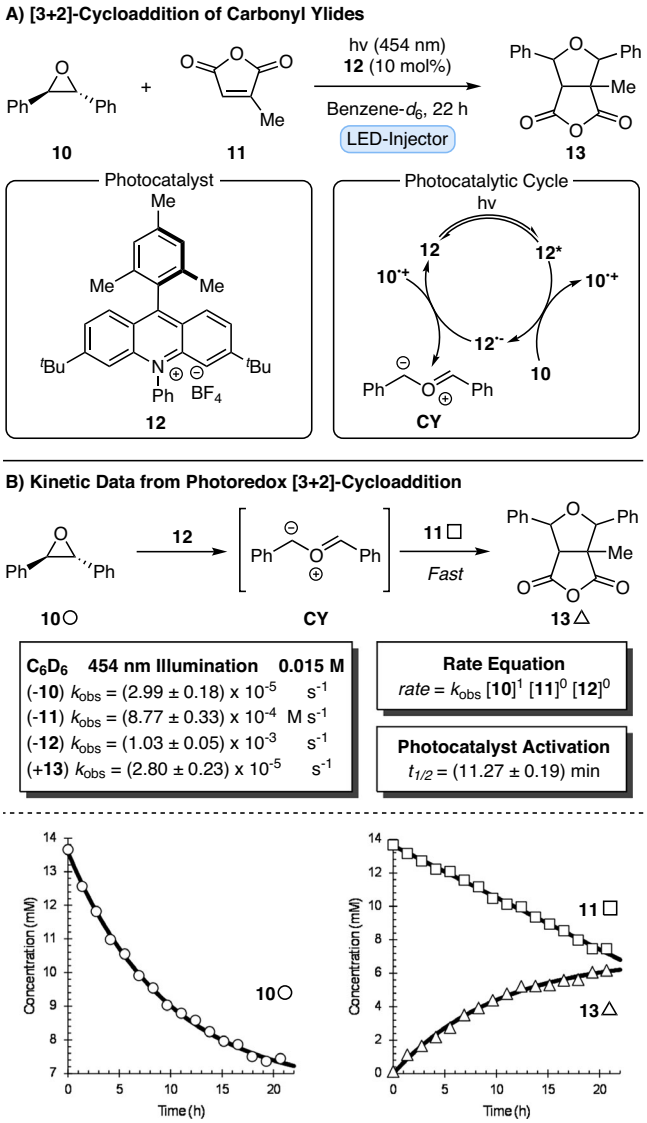

Fig. 8 | [3 + 2]-Cycloaddition of a carbonyl ylide. A Reactions were conducted using 2 mL of dry, degassed benzene-d_6 in a 10 mm NMR tube. Samples were prepared inside of an argon glovebox by adding to the NMR tube *trans*-stilbene oxide **10** (30 µmol, 1.0 equiv.), citraconic anhydride **11** (30 µmol, 1.0 equiv.), photocatalyst **12** (3 µmol, 0.10 equiv.), and 1,1,2,2-tetrachloroethane (30 µmol) as an internal standard. **B** Kinetic data for the photoredox neutral [3 + 2]-cycloaddition reaction. Kinetic data are an average of duplicate runs; negative signs indicate consumption of starting material; positive signs indicate formation of products; solid lines indicate theoretical fit (first order and zeroth order) calculated using the CurveFitter toolbox in Matlab at a 95% confidence interval. Kinetic formulas and fit parameters are available in the Supplementary Information under Section 3: Experiment 1.

concentrations independently. The decay of stilbene oxide **10** followed a first-order kinetic model under pseudo-steady-state conditions ($k_{obs} = 2.99 \pm 0.18 \times 10^{-5}$ s^{-1}) and was found to exhibit a first order dependence on the reaction (Fig. 8B). Of note, upon varying the concentration of citraconic anhydride **11** from 13 to 43 mM the rate of the reaction was found to not be affected and is consistent with a zero-order dependence. The determination of overall rate equation was determined to be $rate = k_{obs}[\mathbf{10}]^1[\mathbf{11}]^0[\mathbf{12}]^0$ (The orders of reagents were determined to be first order in 1, zero order in 2, and zero order in catalyst 3. See SI for details), which indicates that the generation of the carbonyl ylide **CY** is likely rate-determining (Fig. 8B). With the illumination aspect of the LED-RI-NMR system proven successful, our investigations switched to examining the injection aspect of the system (Figs. 9, 10).

Although the generation of synthetic intermediates in situ is operationally simple for bench settings it often becomes logistically challenging for mechanistic investigations due to engineering a reliable delivery system that accurately transfers precise quantities of reagents at a known time and temperature. Therefore, our focus switched to investigating a Wolff rearrangement that requires illumination to generate a synthetic intermediate (ketene) followed by the injection of a subsequent reagent to explore its chemical reactivity.

The irradiation of diazoketones into ketenes and their subsequent reactions has been extensively utilized in various synthetic applications[29,30]. Numerous studies on the Wolff Rearrangement have provided evidence for both concerted and stepwise mechanisms for the 1,2-rearrangment following loss of dinitrogen[31]. The utility of ketenes produced has been exemplified in various recent total syntheses and cycloaddition strategies[32,33]. While the conversion of diazoketones to ketenes has been studied thermally and photochemically, the ability to subsequently investigate the reactivity of the ketene intermediate with nucleophiles is challenging because of the incompatibilities between diazoketones and nucleophiles. As a result, we became interested in these processes and saw it as an opportunity to test the rapid-injection component of the LED-RI-NMR system where we could photochemically generate a reactive ketene and subsequently investigate its capture with alcohols and amines for the synthesis of esters and amides – mimicking bench settings.

We first started with 3-diazo-3-phenylacetone **14** in dry $CDCl_3$ and began irradiation (454 nm) at 25 °C such that the ^{1}H NMR signals could be monitored. A first-order decay of **14** and formation of ketene **15** was observed with k_{obs} values of ($5.35 \pm 0.16 \times 10^{-4}$ s^{-1}) and ($4.77 \pm 0.16 \times 10^{-4}$ s^{-1}), respectively, indicating that the decay of **14** and formation of **15** coincide. Of note, the photogenerated ketene **15** was stable in solution at 25 °C with no detectable change to the ^{1}H NMR spectrum over extended periods of time (>1 h). With the ketene **15** prepared cleanly inside the NMR probe, our investigations switched to probing its chemical reactivity by injecting nucleophiles.

Initially, we sought to compare the reactivity of ketene **15** with methanol versus diethyl amine (Et_2NH); however, upon injection of 1.0 equiv of MeOH into a $CDCl_3$ solution of **15** no reaction occurred[34]. Even upon heating the sample to 60 °C no reaction proceeded and **15** remained unchanged. In a separate case, the injection of diethylamine induced a rapid reaction with **15** and generated the corresponding amide **16** following a second order model ($k_{obs} = 21.91 \pm 0.54$ M^{-1} s^{-1}). Upon, varying the concentration of diethylamine from 8 mM to 20 mM an order dependence of one was observed[35]. In addition, ketene **15** was found to exhibit a first-order dependence on the reaction – providing the following rate equation $rate = k_{obs}[\mathbf{15}]^1[Et_2NH]^1$.

The LED-RI-NMR system enabled us to conduct the Wolff rearrangement entirely within the NMR spectrometer, allowing for real-time monitoring of ketene **15** and enabling reagent injections to probe reactivity. At this point, we have utilized each component (LED incorporation and rapid-injection) separately; however, an advantage to the LED-RI-NMR system is the ability to use these components simultaneously to capture photochemical intermediates.

With the successful demonstration of the illumination and injection features in tandem, our investigations became focused on exploring the injection of reagents while the sample was under constant illumination. Therefore, we chose to investigate a photostationary state or light-induced pre-equilibrium, such that we could investigate the chemical reactivity of one species selectively. In recent years, the photoinduced isomerization of azobenzenes has gained considerable interest in various fields, such as photoswitches and phototherapies, making it an ideal and important system to investigate[36–39].

Irradiation of *trans*-**17** initiates the isomerization into *cis*-**17** until equilibrium is reached; the subsequent ratios of *trans*-/*cis*-**17** is

https://doi.org/10.1038/s41467-025-63848-7

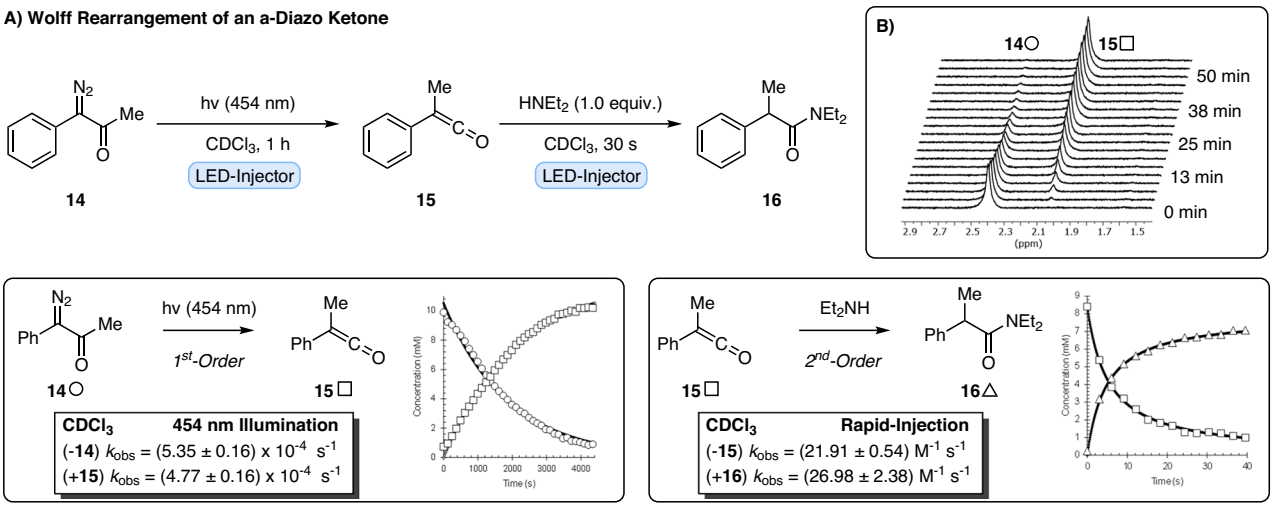

Fig. 9 | Photoinduced Wolff rearrangement. A Reactions were conducted using 2 mL of dry chloroform-*d* in a 10 mm NMR tube. Samples were prepared by adding 3-diazo-3-phenylacetone **14** (30 µmol, 1.0 equiv.) and 1,1,2,2-tetrachloroethane (30 µmol) as an internal standard to the NMR tube and dissolved in dry $CDCl_3$ (2 mL). The sample was illuminated with 454 nm light using the LED-RI-NMR injector system for ca. 1 h at which point all **14** was consumed. Diethylamine (30 µmol, 1.0 equiv.) was then promptly injected via LED-RI-NMR syringe pump (500 µL, 14 mL/min). Kinetic data are an average of duplicate runs; negative signs indicate consumption of starting material; positive signs indicate formation of products; solid lines indicate theoretical fit (first order and second order) calculated using the CurveFitter toolbox in Matlab at a 95% confidence interval. Kinetic formulas and fit parameters are available in the Supplementary Information under Section 3: Experiment 2 **B** Stacked ^{1}H NMR array of the aliphatic region for the conversion of **14** to **15** under 454 nm illumination.

dependent on the wavelength of light used[40]. Reactions of *cis*-**17** that are not competitive with *trans*-**17** are relatively rare, with only a few photoinduced examples in the literature[41,42]. Notably, the [2 + 2]-cycloaddition of *cis*-**17** with ketenes has been reported, where *trans*-**17** does is unreactive[43]. Given our ability to generate ketenes from diazoketones, as shown in the previous example, we saw this as a prime opportunity to study this reaction. First, we needed to determine the photostationary state of **17** and the *trans*-/*cis*- ratio following visible light illumination. A small portion of *trans*-**17** absorbs blue light (380–500 nm), and illumination at 454 nm in $CDCl_3$ using the LED-RI-NMR system yielded a 75:25 *trans*-/*cis*-**17** ratio after approximately 10 min. Both the decay of *trans*-**17** and formation of *cis*-**17** followed a first-order equilibrium model ($K_{eq} = 0.25 \pm 0.01$) until the photostationary state was reached. Once equilibrium was reached, **14** was promptly injected into the sample with the light on. Initially, minor spectral changes were observed, but over 8 h, a clear conversion of **14** and **17** was observed into the corresponding cycloaddition product **18**.

There are several points to be made about the reaction, particularly with how each reagent is involved in the production of **18**. First, upon irradiation of **14** at 454 nm, the Wolff Rearrangement occurs, generating ketene **15**. However, because **15** rapidly undergoes cycloaddition with *cis*-**17**, it is consumed as soon as it is generated. The decay of **14** proceeds in a first-order model ($k_{avg} = 1.14 \pm 0.03 \times 10^{-4}$ s^{-1}) as shown in earlier experiments; however, due to other reagents that absorb light in the reaction medium, the rate of diazo decay is slightly diminished. Second, *trans*-**17** decays in the reaction following a first-order model ($k_{avg} = 3.89 \pm 0.12 \times 10^{-4}$ s^{-1}) akin to the consumption of *cis*-**17** via the photostationary state between *trans*-/*cis*-**17**. As predicted, *trans*-**17** does not participate in the [2 + 2]-cycloaddition but rather acts as a source of *cis*-**17**. Third, the cycloaddition product **18** is formed following a pseudo-first-order model ($k_{avg} = 4.30 \pm 0.15 \times 10^{-4}$ s^{-1}). We rationalize this model to the low concentration of ketene at any given time in the sample. Finally, *cis*-**17** follows a pseudo-first-order kinetic model ($k_{avg} = 3.32 \pm 0.12 \times 10^{-4}$ s^{-1}) where it retains the same 75:25 ratio with *trans*-**17** under equilibrium conditions.

In conclusion, we have developed an LED-RI-NMR system that can be utilized for a variety of mechanistic investigations involving light and reactive intermediates. We have designed this apparatus to be simple and practical for academic and industrial laboratories for the study of photoinduced and photocatalytic reactions, photosensitive proteins[44], and for the discovery of new chemical reactions initiated by light. We have exemplified the utility of this system by studying three different photo-driven reactions that employ different aspects of the LED RI-NMR system. We foresee that this system is advantageous to both LED NMR and RI-NMR systems separately and stands on its own for new mechanistic investigations. We will continue to use this system for the development of new chemical reactions as well as develop new RI-NMR systems for the modern age of chemistry.

Methods

Assembly of the LED-RI-NMR System

To assemble the LED RI-NMR system, first, the injector casing and height-adjusting handle were connected tightly. The LED and injector lines were fed through the injector casing. The injector tip assembly was assembled by threading both glass capillaries through the holes at the end of the assembly until the LED capillary was 19 cm long from the base of the assembly and the injector tip was 9 cm long. These capillaries were secured using the Teflon hex screws to hold them in place. Caution: over-tightening these hex screws can exert significant tension on the capillaries and may cause them to break. We recommend lightly tightening these screws. Once secured, the injector tip assembly was connected to the casing, and the height was adjusted by the handle accordingly. The LED capillary was approximately 2 cm above the bottom of the NMR sample.

Injection operation of the LED-RI-NMR system

When preparing to perform a rapid injection experiment with the LED RI-NMR system, solvent was loaded into the injection line using a 5 mL Normject syringe until solvent was coming out of the capillary. This syringe was connected to a Harvard Apparatus syringe pump set to 12 mL/min for a 0.5 mL total volume infusion. The injection reagent was loaded into the injector tip approximately 10 cm from the end using either a 10 µL or 100 µL Hamilton gastight syringe. The NMR sample was transferred to the spectrometer with the cap off, the LED RI-NMR system was lowered carefully into the sample, and spinning of the NMR sample was turned on to 6 Hz. Spectra were collected first

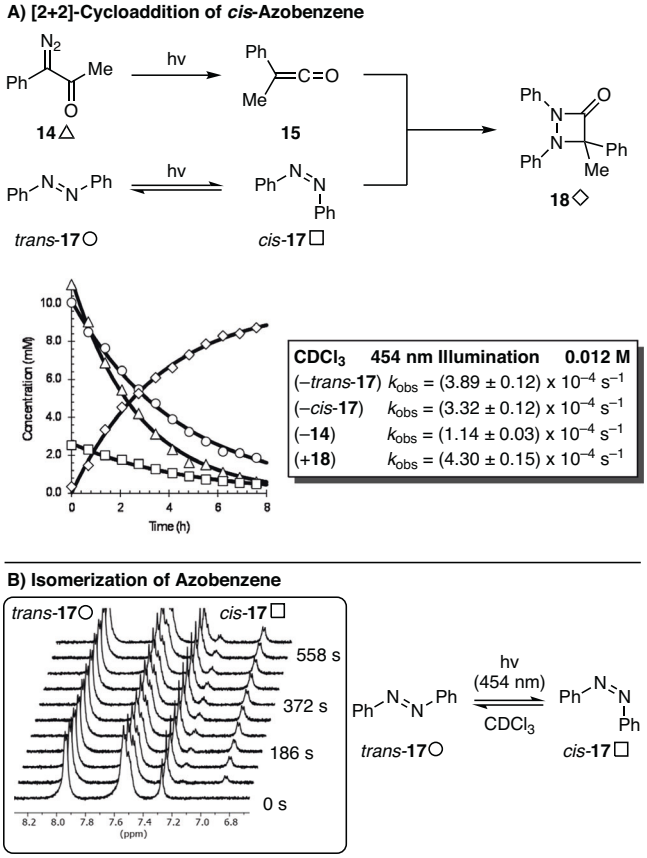

Fig. 10 | Azobenzene isomerization and [2 + 2]-cycloaddition with a ketene. **A** Reactions were conducted using 2 mL of dry chloroform-*d* in a 10 mm NMR tube. Samples were prepared by adding *trans*-**17** (30 μmol, 1.0 equiv.), 1,1,2,2-tetrachloroethane as an internal standard (30 μmol) to the NMR tube and dissolved in $CDCl_3$ (2 mL). The sample was illuminated with 454 nm light using the LED-RI-NMR injector system for ca. 10 min at which point equilibrium was reached between *trans*-**17** and *cis*-**17**. 3-diazo-3-phenylacetone **14** (30 μmol, 1.0 equiv.) was then promptly injected via LED-RI-NMR syringe pump (500 μL, 14 mL/min) with simultaneous 454 nm illumination. Kinetic data are an average of duplicate runs; negative signs indicate consumption of starting material; positive signs indicate formation of products; solid lines indicate theoretical fit (first order) calculated using the CurveFitter toolbox in Matlab at a 95% confidence interval. Kinetic formulas and fit parameters are available in the Supplementary Information under Section 3: Experiment 3. **B** Stacked ^{1}H NMR array of the aromatic region of the isomerization from *trans*-**17** to *cis*-**17**.

with the light off. Once the light was turned on, the photochemical reaction was initiated, and the injection could begin at any time by pressing start on the syringe pump. We have provided a Supplementary Video 1 for a visual of how this operation works in real time using MeOH and blue food coloring dye. Upon completion of the experiment, the injector was removed from the spectrometer with the light off. All kinetic data presented herein are averages of two runs.

Data availability

The schematics and calibration of the LED-RI-NMR system, and the kinetic data generated in this study, are provided in the Supplementary Information file. Source data for the injection calibration and kinetic studies are publicly available in the Figshare database. https://doi.org/10.6084/m9.figshare.29822189.

References

1. Holzgrabe, U. Quantitative NMR spectroscopy in pharmaceutical applications. *Prog. Nucl. Magn. Reson. Spectrosc.* **57**, 229–240 (2010).
2. Crockett, M. P. et al. Breaking the tert-Butyllithium contact ion pair: a gateway to alternate selectivity in lithiation reactions. *J. Am. Chem. Soc.* **145**, 10743–10755 (2023).
3. Christianson, M. D., Tan, E. H. P., Landis, C. R. & Stopped-Flow, N. M. R. Determining the kinetics of [*rac*-(C_2H_4(1-indenyl)$_2$)ZrMe][MeB(C_6F_5)$_3$]-catalyzed polymerization of 1-Hexene by direct observation. *J. Am. Chem. Soc.* **132**, 11461–11463 (2010).
4. Foley, D. A. et al. *Anal. Chem.* **86**, 12008–12013 (2014).
5. Denmark, S. E., Williams, B. J., Eklov, B. M., Pham, S. M. & Beutner, G. L. Design, Validation, and Implementation of a Rapid-Injection NMR System. *J. Org. Chem.* **75**, 5425–5437 (2010).
6. Kidd, J. B. et al. Enantioselective Paternò–Büchi reactions: strategic application of a triplet rebound mechanism for asymmetric photocatalysis. *J. Am. Chem. Soc.* **146**, 15293–15300 (2024).
7. Rickertson, D. R. L. et al. Acridine/Lewis acid complexes as powerful photocatalysts: a combined experimental and mechanistic study. *ACS Catal.* **14**, 14574–14585 (2024).
8. Swords, W. B., Chapman, S. J., Hofstetter, H., Dunn, A. L. & Yoon, T. P. Variable temperature LED-NMR: Rapid insights into a photocatalytic mechanism from reaction progress kinetic analysis. *J. Org. Chem.* **87**, 11293–11295 (2022).
9. Wise, D. E. et al. Photoinduced oxygen transfer using nitroarenes for the anaerobic cleavage of alkenes. *J. Am. Chem. Soc.* **144**, 15437–15442 (2022).
10. Woo, J. et al. Scaffold hopping by net photochemical carbon deletion of azaarenes. *Science* **376**, 527–532 (2022).
11. Feldmeier, C., Bartling, H., Riedle, E. & Gschwind, R. M. LED based NMR illumination device for mechanistic studies on photochemical reactions – Versatile and simple, yet surprisingly powerful. *J. Mag. Reson.* **232**, 39–44 (2013).
12. Ji, Y. et al. Spectroscopy: A practical tool for mechanistic studies of photochemical reactions. *ChemPhotoChem* **3**, 984–992 (2019).
13. Seegerer, A., Nitschke, P. & Gscwind, R. M. Combined in situ illumination-NMR-UV/Vis Spectroscopy: A new mechanistic tool in photochemistry. *Angew. Chem. Int. Ed.* **57**, 7493–7497 (2018).
14. Foley, D. A. et al. ReactNMR and ReactIR as reaction monitoring and mechanistic elucidation tools: The NCS mediated cascade reaction of α-Thioamides to α-Thio-β-chloroacrylamides. *J. Org. Chem.* **76**, 9630–9640 (2011).
15. Chu, C. et al. Implementation of laser flash photolysis for radical-induced reactions and environmental implications. *Water Res.* **244**, 120526–12040 (2023).
16. Thomas, A. A. & Denmark, S. E. Pre-transmetalation intermediates in the Suzuki-Miyaura reaction revealed: The missing link. *Science* **352**, 329–332 (2016).
17. Bertz, S. H. et al. Rapid injection NMR reveals η3 'π-Allyl' CuIII intermediates in addition reactions of organocuprate reagents. *J. Am. Chem. Soc.* **134**, 9557–9560 (2012).
18. McGarrity, J. F., Prodolliet, J. & Smyth, T. Rapid Injection NMR: A simple technique for the observation of reactive intermediates. *Org. Magn. Reson.* **17**, 59–65 (1981).
19. Bertz, S. H. et al. Study of Iodo- and Cyano-Gilman reagents with 2-Cyclohexanone: Observation of π-complexes and their rates of formation. *J. Am. Chem. Soc.* **124**, 13650–13651 (2002).
20. Jones, A. C., Sanders, A. W., Bevan, M. J. & Reich, H. J. Reactivity of Individual Organolithium Aggregates: A RINMR Study of *n*-Butyllithium and 2-Methoxy-6-(methoxymethyl)phenyllithium. *J. Am. Chem. Soc.* **129**, 3492–3493 (2007).
21. Wu, D. et al. Cyclopropenimine-mediated CO_2 activation for the synthesis of polyurethanes and small-molecule carbonates and carbamates. *Angew. Chem. Int. Ed.* **63**, e202401281 (2024).
22. Arriaga, D. K., Kang, S. & Thomas, A. A. Effect of solvent on the rate of ozonolysis: development of a homogeneous flow ozonolysis protocol. *J. Org. Chem.* **88**, 13720–13726 (2023).

23. McMills, M. C.; Wright, D. Carbonyl Ylides. In *Synthetic Applications of 1,3-Dipolar Cycloaddition Chemistry Toward Heterocycles and Natural Products*. The Chemistry of Heterocyclic Compounds, Vol. 59; John Wiley & Sons, 2002; pp 253-314.
24. Alfonzo, E. & Beeler, A. B. A sterically encumbered photoredox catalyst enables the unified synthesis of the classical lignan family of natural products. *Chem. Sci.* **10**, 7746–7754 (2019).
25. Alfonzo, E., Alfonso, F. S. & Beeler, A. B. Redesign of a Pyrylium Photoredox catalyst and its application to the generation of Carbonyl Ylides. *Org. Lett.* **19**, 2989–2992 (2017).
26. Kumar, C. V., Chattopadhyay, S. K. & Das, P. K. Carbonyl Ylides photogenerated from isomeric stilbene oxides. Temperature dependence of decay kinetics. *J. Phys. Chem.* **88**, 5639–5643 (1984).
27. Das, P. K. & Griffin, G. W. Transient spectral and kinetic behaviors of Carbonyl Ylide Photogenerated from 2,2-Dicyano-3-(2-Naphthyl)-Oxirane. *J. Photochem.* **27**, 317–325 (1984).
28. Benniston, A. C. et al. Charge Shift and Triplet State Formation in the 9-Mesityl-10-methylacridinium Cation. *J. Am. Chem. Soc.* **127**, 16054–16064 (2005).
29. Wolff, L. Ueber Diazoanhydride. *Justus Liebigs Ann. Chem.* **325**, 129–195 (1902).
30. Kirmse, W. 100 years of the Wolff rearrangement. *Eur. J. Org. Chem.* **2002**, 2193–2256 (2002).
31. Gill, G. B. The Wolff Rearrangment. In *Comprehensive Organic Synthesis*; Chemistry, Molecular Sciences and Chemical Engineering, Vol. 3; Permagon, 1991, pp 887-912. https://doi.org/10.1016/B978-0-08-052349-1.00085-8.
32. Chapman, L. M., Beck, J. C., Wu, L. & Reisman, S. E. Enantioselective Total Synthesis of (+)-Psiguadial B. *J. Am. Chem. Soc.* **138**, 9803–9806 (2016).
33. Li, M.-M. et al. Sequential visible-light photoactivation and palladium catalysis enabling Enantioselective [4 + 2] Cycloadditions. *J. Am. Chem. Soc.* **139**, 144707–14713 (2017).
34. Allen, A. D. & Tidwell, T. T. Amination of Ketenes: Kinetic and mechanistic studies. *J. Org. Chem.* **64**, 266–271 (1999).
35. Some ketene aminations in polar solvents (MeCN, H_2O, etc.) have shown higher order dependency on the amine concentration; see Allen, A. D.; Stevenson, A., Tidwell, T. T. Hydration Reactivity of Persistent Conjugated Ketenes. *J. Org. Chem.* **54**, 2843-2848 (1989).
36. Jerca, F. A., Jerca, V. V. & Hoogenboom, R. Advances and opportunities in the exciting world of azobenzenes. *Nat. Rev. Chem.* **6**, 51–69 (2022).
37. Kind, J., Kaltschnee, L., Leyendecker, M. & Thiele, C. M. Distinction of *trans-cis* photoisomers with comparable optical properties in multiple-state photochromic systems - examining a molecule with three azobenzenes *via in situ* irradiation NMR spectroscopy. *Chem. Commun.* **52**, 12506–12509 (2016).
38. Čechová, L. et al. Photoswitching Behavior of 5-Phenylazopyrimidines: In Situ Irradiation NMR and Optical Spectroscopy Combined with Theoretical Methods. *J. Org. Chem.* **83**, 5986–5998 (2018).
39. Procházková, E. et al. Photoswitchable Intramolecular Hydrogen Bonds in 5-Phenylazopyrimidines Revealed by In Situ Irradiation NMR Spectroscopy. *Chem. Eur. J.* **24**, 492–498 (2018).
40. Tait, K. M., Parkinson, J. A., Bates, S. P., Ebenezer, W. J. & Jones, A. C. The novel use of NMR spectroscopy with in situ laser irradiation to study azo photoisomerization. *J. Photochem. Photobiol., A.* **154**, 179–188 (2003).
41. Yang, J., Wang, C., Zhou, H., Kong, Q. & Ma, W. Visible-Light-Driven Hydrophosphorylation of Azobenzenes Enabled by *trans*-to-*cis* Photoisomerization. *Adv. Synth. Catal.* **364**, 4275–4280 (2022).
42. Hall, J. H. & Kellogg, R. Synthesis and Thermal Stability of 1,2-Diazetidinones. Reaction of Diphenylketene with Substituted Azobenzenes. *J. Org. Chem.* **31**, 1079–1082 (1966).
43. Ried, W. & Piesch, S. Äthinierungsreaktionen, XXIII. Reaktionen am 11*H*-Dibenzo[*c.f*][1.2]diazepinon-(11). *Chem. Ber.* **99**, 233–238 (1966).
44. Kim, C. et al. Structural dynamics of protein-protein association involved in the light-induced transition of Avena sativa LOV2 protein. *Nat. Commun.* **15**, 6991 (2024).

Acknowledgements

AAT, DKA, and RK are thankful for the generous financial support from the Welch Foundation (A-2081-20240404) and Texas A&M University for the construction of the LED-RI-NMR system. AAT, DKA, and RK are grateful to the U.S. National Science Foundation (CAREER-2238881), which supported our mechanistic studies.

Author contributions

A.A.T. conceived the work. A.A.T., D.K.A. and R.K. designed the experiments. D.K.A. designed, machined, and constructed the components for the LED-RI-NMR system, as well as calibrated the injection and illumination features. D.K.A. and R.K. conducted all LED-RI-NMR kinetic experiments. DKA processed all kinetic data. D.K.A. synthesized compounds **10** and **18**. R.K. synthesized compound **15** and precursors thereof. AAT and DKA wrote the manuscript.

Competing interests

The authors declare the following competing interest(s): AAT and DKA are in the process of filing a patent on the design and construction of the LED-RI-NMR system. The remaining authors declare no competing interests.

Additional information

Supplementary information The online version contains supplementary material available at https://doi.org/10.1038/s41467-025-63848-7.

Correspondence and requests for materials should be addressed to Andy A. Thomas.

Peer review information *Nature Communications* thanks Mikhail Reibarkh and the other anonymous reviewer(s) for their contribution to the peer review of this work. A peer review file is available.